Carbohydrate Polymers 108 (2014) 321–330

Contents lists available at ScienceDirect

Carbohydrate Polymers

journal homepage: www.elsevier.com/locate/carbpol

Crosslinker effects on functional properties of alginate/N-succinylchitosan based hydrogels

Maria Cristina Straccia[a], Ida Romano[b], Adriana Oliva[c], Gabriella Santagata[a,*], Paola Laurienzo[a]

[a] Institute of Chemistry and Technology of Polymers, CNR, via Campi Flegrei 34, 80078 Pozzuoli, Naples, Italy
[b] Institute of Biomolecular Chemistry, CNR, via Campi Flegrei 34, 80078 Pozzuoli, Naples, Italy
[c] Department of Biochemistry, Biophysics and General Pathology, Second University of Naples, via L. De Crecchio 7, 80138 Naples, Italy

ARTICLE INFO

Article history:
Received 30 October 2013
Received in revised form 13 February 2014
Accepted 16 February 2014
Available online 22 February 2014

Keywords:
Alginate
N-succinylchitosan
Cellulose microfibers
Antibacterial activity
Zinc cytotoxicity
Wound dressing

ABSTRACT

In this paper, physico-chemical, mechanical and antimicrobial properties of hydrogels based on alginate/N-succinylchitosan blends crosslinked by calcium or zinc ions containing cellulose microfibers were investigated and discussed. With respect to plain alginate hydrogels, the addition of N-succinylchitosan significantly improved properties such as swelling degree and stability in saline solution. The water vapour transmission rate confirmed that all the hydrogels were able to assure a moist wound environment. Morphological analysis showed a good embedding of fibres within the zinc crosslinked hydrogels. In addition, zinc-crosslinked hydrogels evidenced antimicrobial activity against two common skin pathogenic bacteria, *Staphylococcus aureus* and *Escherichia coli*. Cytotoxicity assays proved that the amount of zinc released is slightly over the toxic level. Overall, the characteristics of the zinc-crosslinked hydrogels showed their potential interest as materials for wound dressing.

1. Introduction

Hydrogels based on natural polysaccharides have been largely investigated in pharmaceutical and medical fields, as tissue engineering (Vlierberghe, Dubruel, & Schacht, 2011), drug delivery (Boateng, Matthews, Stevens, & Eccleston, 2008), immobilization of cells and enzymes. The use of hydrogels as wound dressing materials in the healthcare industry is well documented in literature (Pudner, 2001; Werner & Grose, 2003) Hydrogels have the function to absorb the exuding liquids and debris from the wound area. Additionally, they allow the gaseous exchange to the wound surface while supplying water molecules to the wound bed, induce beneficial cooling effects in case of burn wounds, avoid trauma or pain during dressing change, and moreover their transparency allows the observation of the status of the injured zone. Hydrogels can be applied as such or as a solid, soft-elastic thin film (sheet) (Peng, Lin, Wang, & Wu, 2012). Among others, hydrogel based on alginate (A) find large applications for the treatment of chronic and exuding wounds, due to their high absorbency that limit wound secretions, minimize bacterial contamination and accelerate epithelialization and healing, once provided that the underlying pathology is treated (Chan, Whitney, & Neufeld, 2009; Hoffman, 2012; Ovington, 2007). Due to the high water absorbency, they are not indicated for dry wounds. Sodium alginate is a water soluble linear polysaccharide extracted from brown seaweeds. It is a copolymer of 1–4 linked α-L-guluronate (G) and β-D-mannuronate (M) residues in varying proportions, able to form hydrogels by ionic interaction with divalent cations, usually Ca^{2+}.

Alginates from different sources are characterized by different relative amounts and length of regions composed of sequential G units (G block), sequential M units (M block) and randomly alternated G and M units (MG block). Calcium crosslinked gels degrade slowly, and the released calcium ions were shown to increase the proliferation of fibroblasts (Doyle, Roth, & Smith, 1996; Lay-Flurrie, 2004), activate the production of factor-α, responsible of the inflammatory signals accounting for the healing process (Thomas, Harding, & Moore, 2000), and promote the haemostasis in the first stage of wound healing (Lansdown, 2002). In addition, due to sodium-calcium ion exchange, hydrogels are easily rinsed away with saline irrigations. Alginate dressings are available in form of freeze-dried porous sheets useful for flat wounds, or as flexible fibres and gels employed in case of deep lesions.

* Corresponding author. Tel.: +39 0818675214; fax: +39 0815235230.
E-mail addresses: mariacristina.straccia@ictp.cnr.it (M.C. Straccia), iromano@icb.cnr.it (I. Romano), adriana.oliva@unina2.it (A. Oliva), paola.laurienzo@ictp.cnr.it (G. Santagata), santagata@ictp.cnr.it (P. Laurienzo).

http://dx.doi.org/10.1016/j.carbpol.2014.02.054
0144-8617/

Hydrogels obtained by blending alginate with other biopolymers, such as hyaluronic acid (Na, Oh, Song, & Lee, 2012), collagen (Donaghue et al., 1998) and chitosan (Pandima Devi et al., 2012) have been widely investigated. Chitosan draws particular attention as drug carrier and antibacterial agent, due to intrinsic and unique biochemical properties (Muzzarelli, 2009). However, the application of chitosan is limited owing to its water insolubility at neutral pH. To overcome this drawback, chitosan has been chemically modified by substitution of part of amines with various hydrophilic groups, usually with a negative charge, in order to realize water-soluble derivates. Among them, N-succinylchitosan (sCH), obtained by introduction of succinyl groups onto glucosamine units, shows interesting in vitro and in vivo properties (Yamaguchi, Arai, Itoh, & Hirano, 1981), although it lacks in antimicrobial activity (Kong, Chen, Xing, & Park, 2010). Finally, it is worth to highlight that literature data accounts for several wound dressing biomaterials based on synergic cooperation of hydrogels and textile fibres (Abdelrahman & Newton, 2011; Raghavendr et al., 2013). The inclusion of cellulose enhances the durability of the dressings during the repair process, thus promoting the skin regeneration and ensuring a suitable balance between flexibility and rigidity (Grace, Chand, & Bajpai, 2009; Khan, Peh, & Ch'ng, 2000; Sakchai, Chureerat, & Srisagul, 2006). A possible disadvantage of fibrous dressings is that fibres can be released and can stick to the wound, causing pain during dressing changes.

Up to now, research about alginate and N-succinylchitosan based hydrogels has been focused on several topics (Ayala, De Rosa, Laurienzo, & Malinconico, 2007; Li, Dai, Zhang, Wang, & Wei, 2008) not including wound dressing. In the present work, hydrogels based on sodium alginate (A), N-succinyl chitosan (sCH) and/or cellulose microfibers (F) have been realized and their chemical-physical properties, mechanical performances and antimicrobial activity were assessed. Finally, in order to investigate on possible cytotoxic effects of released zinc ions, in vitro assays using human mesenchymal stromal cells (MSCs) were reported.

2. Experimental

2.1. Materials

Sodium alginate (A), purchased from Lianyungang Zhongda Seaweed Industrial Co. Ltd. (XuGou, Lianyungang, Jiangsu, China), was characterized by 37 ± 1% of G residues. The weight average molecular weight (M_W) was 1.2×10^6 Da and the number average molecular weight (M_N) corresponded to 2.3×10^5 Da. N-succinylchitosan (sCH), a water soluble chitosan, was supplied by Fu Zhou Corona Science & Technology Development Co., Ltd. (FuZhou, FuJian Province, PR China). It showed an average molecular weight (M_W) of 3×10^5 Da. The degree of succinylation, defined as the molar ratio between the N-succinyl groups and the repeating units of glucosamine, was 0.90. Agar, purchased from Oxoid Ltd. (Hampshire, UK), was used as culture medium. Pure cellulose microfibers (F) were kindly provided by the International Paper Company (Bastrop, Louisiana, USA). These fibres were of 1–4 mm in length and about 15 μm in diameter. Zinc chloride (J.T. Baker, Avantor Performance Materials, Milan, Italy) and calcium chloride (Sigma Aldrich, Milan, Italy) were analytical reagent grade and used as received.

2.2. Film preparation

Films of plain polymers and blends were prepared by casting from 1% (w/v) aqueous solutions. To prepare blends films, A and sCH were dissolved separately in freshly distilled water and then merged. The solutions were, kept few minutes under vacuum to remove bubbles, then gently poured into a polyester Petri dish placed under a ventilated hood until complete water evaporation. Fibrous films (A/F; sCH/F; A/sCH/F) were prepared by dispersing the cellulose microfibers (25% by wt with respect to the polymers) in the polymeric solutions through vigorous mechanical stirring for 3 h.

2.3. Crosslinking and swelling kinetics

Crosslinking by external gelation was performed by dipping the films in 150 mL of 1% or 3% (w/v) calcium or zinc chloride water solutions for 180 min. These two salt concentrations were chosen as, respectively, the minimum and the maximum concentration in order to obtain high degree of cross-linking throughout the film. Before testing, all samples were dried in an oven under vacuum at 60 °C for 24 h, and the average thickness was measured by using a micrometre (Digital Micrometer Mitutoyo IP-65, Japan). At least five thickness readings from different regions of each film were taken. In order to follow the swelling kinetics, films were recovered by filtration, washed one time by dipping in 100 mL of deionised water for five minutes to remove the excess of salt, withdrawn by briefly blotting between two filter papers, and then weighed. The swelling was monitored by measuring the water up-take as a function of time. Water sorption percentage was determined using the following empirical equation:

$$W_{st}\% = \left(\frac{W_t - W_d}{W_d}\right) \times 100 \quad (1)$$

where W_{st} was the water sorption of the films, W_d and W_t respectively were the weights of the dried and swollen films at different times. Measurements were performed in triplicate and average data were used for calculations.

2.4. Stability test

In order to examine the stability of crosslinked films, a test in normal saline solution (NaCl 0.9%, w/v) was performed. Films were first dried in an oven at 60 °C for 24 h under vacuum, then weighed and placed in 50 mL of normal saline solution at room temperature. At set time intervals, the samples were recovered by filtration, withdrawn by briefly blotting between two filter papers, dried as previously described, then weighed. Weight loss (ΔW) was expressed as percentage using the following equation:

$$W\% = \left(\frac{W_t - W_0}{W_0}\right) \times 100 \quad (2)$$

where W_t and W_0 were the weights at time t and time 0, respectively. All measurements were performed in triplicate and average data were reported.

2.5. Water vapour transmission rate (WVTR)

Water vapour transmission rate (WVTR) was measured according to the ASTM E96 wet method (ASTM, 1993), using a CEAST metal cup with a 706.5×10^{-6} m^2 exposed area. Cups were placed in an environmental chamber set at a temperature of 25 °C and a relative humidity of 50%; each sample was first equilibrated for 48 h before measurements, then weighed every 24 h for 5 days. WVTR values were expressed in g (h m^2)$^{-1}$ and determined with graphic analysis method following the equation:

$$WVTR = \frac{\Delta G}{t \times A} \quad (3)$$

where ΔG was the weight change (g), t was the time during which G occurred (h), A was the test area cup (m^2) and $\Delta G/t$ was the slope

of strains line ($g\,h^{-1}$). Data are the mean of three measurements for each sample.

2.6. Mechanical properties

Tensile tests were performed by means of a dynamometer model 5564, Instron (Canton, USA) equipped with a 1 kN load cell. The measurements were performed on dumbbell-shaped films; the width and the length of specimens were respectively 5 and 44 mm, while the thickness of each film was measured at five random points using a micrometre and the result was expressed as the average value. For the test, only films with thickness deviation less than 10% from the mean value were used. Prior to testing, the films were conditioned in an environmental chamber at 25 °C and 50% relative humidity (RH) for 24 h. The tests were performed at 23 ± 2 °C and 45 ± 5% RH, at a clamp separation rate of 2 mm min^{-1}. The reported data are the average values of six measurements.

2.7. Scanning electron microscopy (SEM)

Morphological analysis of film surfaces was performed by means of scanning electron microscopy (SEM) (Quanta 200 FEG, 338 FEI, Eindhoven, The Netherlands). Samples were fixed onto aluminium stubs through carbon adhesive disks and observed in high vacuum mode using a secondary electron detector and an accelerating voltage of 20.0 kV.

The samples were observed at room temperature and at an internal water vapour pressure of 66.66 Pa. Before observation, samples surfaces were coated with a homogeneous layer (18 ± 0.2 nm) of Au–Pd alloy using a coating device (MED 020, Bal-Tec AG, Tucson, AZ, USA).

2.8. Antibacterial activity

Antibacterial activity was evaluated against the pathogenic gram-positive strain *Staphylococcus aureus* (DSM 1104) and the gram-negative *Escherichia coli* (DSM 8579), purchased from Deutsche Samlug von Mikroorganismen und Zellkulturen GmbH (DSMZ, Germany). The bacteria were respectively grown in Trypticase Soy Broth (TSB) and Luria-Bertani broth (LB) medium (Oxoid Ltd., UK), for 18 h at 37 °C, to obtain isolated colonies. The ASTM standard test method E2149-01 (ASTM, 2001) was used to determine antimicrobial activity of immobilized antimicrobial agents under dynamic contact condition.

The bacterial concentration was determined by measuring the optical density at 600 nm (OD_{600}) by means of a spectrophotometer. After growth and harvesting, the bacterial cells were washed with Ringer Solution (RS), a sterile buffer saline solution, composed of 0.150 g of potassium chloride, 2.25 g of sodium chloride, 0.05 g of sodium bicarbonate and 0.12 g of calcium chloride hexahydrated, *per litre* of solution. The bacterial cells were diluted in RS up to an absorbance of 0.250 ± 0.01, corresponding to a concentration of approximately 1.5–3.0 × 10^8 colony-forming units *per millilitre* ($CFU\,mL^{-1}$). A second dilution was carried out to obtain assays inoculums of about 10^6 $CFU\,mL^{-1}$.

Zinc crosslinked hydrogel specimens (1 cm × 2 cm), were put in conical flasks and sterilized by autoclaving. 10 mL of the working bacterial suspension were added to the samples and placed on a wrist-action shaker, at room temperature. Working bacterial solutions with A-Ca hydrogel were used as negative controls. After fixed contact times, 1 min (t_0), and 24 h (t_{24}), 100 μL of the bacterial suspensions were spread on solid medium in Petri dishes and incubated at 37 °C for 24 h. The average colony count of duplicate plates was used to calculate the $CFU\,mL^{-1}$. Inoculum assay was used as control. All experiments were performed in triplicate and average data were used for calculations. The percentage reduction can be calculated using the following formula:

$$\text{Reduction}\,\%\,(\text{CFU mL}^{-1}) = \left(\frac{B-A}{B}\right) \times 100 \quad (4)$$

where A = $CFU\,mL^{-1}$ for the corning flask containing the sample after specified contact time and B = $CFU\,mL^{-1}$ at "0 h" contact time.

2.9. Atomic absorption spectrometry (AAS)

In order to follow the kinetics of zinc release, film samples (1 cm × 2 cm) were immersed in 10 mL of RS. The amount of zinc released in solution after 20, 40, 60, 1440 (24 h) and 2880 min (48 h) was determined by AAS. For the determination of total zinc content, samples were kept in RS at 60 °C for 48 h on a wrist-action shaker to allow complete dissolution. All the solutions were centrifuged and filtered on paper before analysis, The AAS measurements were performed using a Perkin Elmer Analyst 800 instrument (Norwalk, CT) and AS 90 plus flame autosampler. All the data were recorded and processed by WinLab32 software. A stock zinc solution in 2.5% HNO_3 was used for standard calibration curve. The zinc content was calculated with the following equation:

$$\text{Total zinc content}\,(\text{mg L}^{-1}) = \left(\frac{A_{\text{sample}} \times C_{\text{std}}}{A_{\text{std}}}\right) \times \left(\frac{b}{a}\right) \quad (5)$$

where A_{sample} is the sample absorbance, A_{std} is the absorbance of standard solution, C_{std} ($mg\,L^{-1}$) is the concentration of standard solution, and b/a is the dilution factor. All measurements were performed in triplicate and average data were considered.

2.10. Cell viability tests

Mesenchymal stromal cells (MSCs) were obtained from samples of human bone marrow harvested from healthy donors, after informed consent was provided. MSCs cultures were initiated as described previously (Oliva et al., 2005).

MSCs were seeded in 24-well plates at a density of 50,000/well and treated with increasing concentrations of $ZnCl_2$ from 0 (control) to a maximum of 400 μM. The assay was performed in quadruplicate. After 24 h cell vitality was assessed by PrestoBlue test. This reagent is a cell permeable resazurin-based solution that, when added to cells, is modified by the reducing environment of the viable cells becoming fluorescent. Cells were washed with phosphate buffered saline (PBS) and incubated with 0.5 mL of PrestoBlue 10% solution for 10 min at 37 °C. At the end of this time, the liquid was collected and the cell layer washed once with 0.5 mL of PBS. The fluorescence of the mixture was measured at 560/590 nm fluorescence excitation/emission (Perkin Elmer LS55 Luminescence Spectrometer) and expressed as Relative Fluorescence Units (RFU).

3. Results and discussion

3.1. Crosslinking and swelling kinetics

The external gelation method, consisting in dipping a film or dropping a solution of alginate into a solution of crosslinker, is commonly used to obtain suitable model of wound dressing materials (Goh, Heng, & Chan, 2012). Fig. 1a and b, respectively shows the swelling kinetics of films and fibrous films during crosslinking, either in calcium or in zinc chloride solutions, at two different salt concentrations, namely 1% and 3% (w/v).

Looking at Fig. 1a and b, some outcomes are worthy of considerations. The first noticeable evidence concerns the syneresis of all the samples occurring during swelling. Syneresis is a macroscopic phenomenon characterized by a volume reduction of the gels with

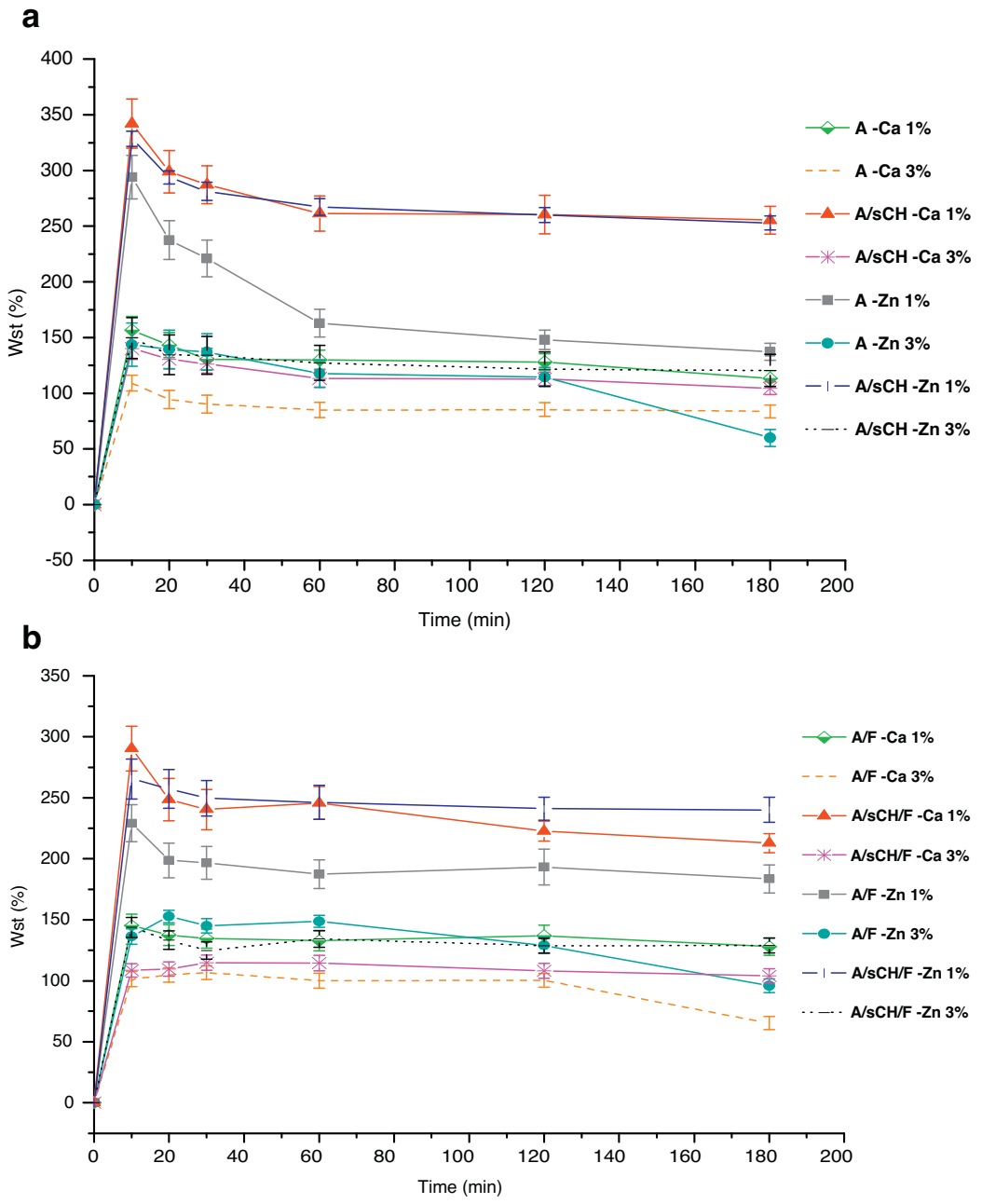

Fig. 1. Water sorption percentage (W_{st} %) as a function of time (min) of films (a) and fibrous films (b) crosslinked in calcium and zinc chloride solution at 1% and 3% (w/v).

the concomitant release of water (Davidovich-Pinhas & Bianco-Peled, 2010). Some authors (Draget, Oestgaard, & Smidsroed, 1990) found that syneresis was strongly related to the amount of calcium ions within the gel. Indeed, in case of an excess of calcium ions syneresis is remarkable. Syneresis degree was also correlated to molecular weight and mobility of the segments between consecutive crosslinked points. Low molecular weight segments formed a more rigid structure, which prevented shrinkage of the gel, thus leading to a low degree of syneresis; on the contrary, longer and more flexible segments allowed rapid relaxation, further facilitating the shrinkage, i.e., high degree of syneresis (Draget et al., 2001). Accordingly, alginate films showed a strong syneresis with either Zn^{2+} or Ca^{2+} at 1%, whereas syneresis was less pronounced at 3%. Moreover, a slower swelling rate at 1% was also observed, as the plateau was achieved after 60 min, against only 30 min in the case of 3%. Syneresis therefore provides information about equilibrium properties of the gel in terms of how fast and how much the junction zones are reorganized.

The swelling degree of all films strongly depended on the cations concentration. In particular, the water up-take resulted lower at higher concentration. This effect was particularly remarkable for blends, where the swelling was halved going from 1% to 3%.

Davidovich-Pinhas and Bianco-Peled (2010), underlined that, in the case of high concentration of cations (>3%), the sudden an abrupt crosslinking of alginate chains on the surface forms a thick layer which acts as a barrier and, in turn, reduces the swelling. Moreover, the diffusion rate of ions through the films decreases and the formation of junction zones in the inner core of the hydrogel is prevented. Therefore the relation between swelling and concentration of crosslinking agent is evident (Kong, Lee, & Mooney, 2003; Omidian, Rocca, & Park, 2006). As a matter of fact, we investigated

also 2% solutions (data not reported) and no relevant differences were found with respect to 3%.

Crosslinking mechanism of sodium alginate has been largely investigated in the case of calcium ions. As calcium ions bind fundamentally to G residues, the process involves preferentially G blocks of the alginate according to "egg-box" model (Grant, Morris, Rees, Smith, & Thom, 1973; Stokke et al., 2000). As concerning the crosslinking mechanism with zinc ions, some authors reported that zinc and calcium cations bind different sites of alginate; in particular, while calcium ions involve only the G blocks, the zinc ions are less selective, providing a more extensive three-dimensional network (Aslani, & Kennedy, 1996a). Pillay and Fassihi (2005) elucidated the different crosslinking mechanism of zinc and calcium ions on the basis of their different crystal structures and coordination numbers. In the case of Zn^{2+}, the peculiar crystal structure, together with the smaller atomic volume and ionic radius, results in a limited impedance to zinc diffusion into the polymeric pockets and in a higher cation content inside the polymeric binding sites. The authors underlined that the higher content of zinc ions inhibits water molecules to permeate into the polymeric network, reducing the swelling. For this reason, zinc crosslinked alginate hydrogels are commonly used in controlled drug release systems to reduce the rate of release of encapsulated drugs (Chan, Jin, & Heng, 2002; Jay & Saltzman, 2009). Nevertheless, Fig. 1a evidenced that, in plain alginate, Zn^{2+} induced a swelling degree higher than Ca^{2+}, and this trend was even more pronounced at 1%. This outcome can be explained considering that swelling occurred during the crosslinking. As previously described by Russo, Malinconico, and Santagata (2007), sodium alginate films, when dipped in water solutions of calcium chloride, swell and at the same time crosslink; for this reason, the conformations of the swelled films are stabilized by the concurrently forming junction zones between macromolecular chains, in this way providing the absorption and the holding of some water inside the polymeric network. This hypothesis was confirmed by the increase of thickness, measured after drying, of crosslinked films with respect to the initial ones. It followed that a higher number of crosslinking points resulted in higher swelling. We really found a similar increase of the thickness in all films and fibrous films upon crosslinking, after just 10 min of dipping, with either calcium or zinc chloride solutions; according with the results of Russo et al. (2007) this thickness increase was followed by a fairly regular trend during which the samples preserved their stable conformations (data not shown). We can conclude that the more extensive crosslinking area in the case of zinc, due to its lack of selectivity, was responsible of the higher swelling degree.

In the blends, the factors which affected the extent and uniformity of crosslinking were the relative binding affinity as well as the binding selectivity of the cations towards alginate. As shown, the overall water percentage up-take was almost twice than that of plain alginate in the case of crosslinking with 1% solutions for both calcium and zinc, while no significant differences were found with 3% solutions. The effect of the addition of sCH was particularly evident in the blends crosslinked with zinc, that showed decreased syneresis, higher values of swelling and faster equilibrium achievement with respect to neat alginate. A and sCH, being two polysaccharides, are miscible. The molecular miscibility between the blends components was supported by the evaluation of glass transition temperatures of neat polymers and their blends; the presence, in the blends, of a single Tg, whose value lies between those of the pure polymers, was plainly indicative of molecular miscibility (Hyun-Jung, Kyung-Soo, & Seung-Taik, 2004, see Table S1 in Supplementary data). In particular, A and sCH form a semi-interpenetrating polymer network, in which sCH is physically entrapped in the alginate three-dimensional structure at a molecular level. As a matter of fact, Nobile, Pirozzi, Somma, Gomez d'Ayala, and Laurienzo (2008) and Gomez d'Ayala, De Rosa, Laurienzo, and Malinconico (2007) showed that sCH can be involved in the crosslinking through the succinyl groups. Moreover, since the high succinylation degree of sCH (90%), it is plausible to hypothesize that the number of free amine groups available to the formation of polyelectrolyte complex with A is negligible. As a consequence of all these considerations, we may hypothesize that at 3% a partial cross-linking of sCH occurs, so the swelling behaviour of the gel is similar to that of plain A, while at 1% the presence of un-crosslinked sCH chains renders the network looser, so the gel swells more.

Fig. 1b reports the swelling kinetics of fibrous films. A slight decrease of swelling degree and syneresis was detected, since the strong intermolecular interaction between polymers and fibres, induced both a reduction of the water sorption content and a decreasing of the de-swelling process (Karaaslan, Tshabalala, & Buschle-Diller, 2012). For this reason the swelling plateau, following the squeezing out of water after syneresis, was achieved faster. The addition of fibres could be so considered useful for both reducing undesirable syneresis and inhibiting the film shrinkage.

3.2. Stability test

Stability test of crosslinked films was performed in normal saline solution, as biological wound fluids cannot be adequately simulated by any standard medium, and wound pH depends on bacterial colonization. The weight loss in normal saline solution is generally considered as an index of instability of crosslinked films. In presence of univalent ions, as sodium, the divalent/monovalent ions exchange causes the hydrogel collapse with consequent release of un-crosslinked polymers in solution, with decrease of weight (Goh, Heng, & Chan, 2012). On the basis of swelling behaviour reported above, only films crosslinked with 1% Ca^{2+}or Zn^{2+}solution were tested, and 120 min was set as overall crosslinking time.

In Fig. 2a and b the weight loss percentage ($\Delta W\%$) of films and fibrous films as a function of dipping time is reported.

The stability test showed that A-Ca and A-Zn samples behave in a similar way up to 180 min, evidencing 10% weight loss within 60 min, and fairly 20% within 180 min (Fig. 2a). After 1440 min, A-Zn lost around 40% weight, while A-Ca was stable.

As concerning the blends, while A/sCH-Zn film evidenced a stability very close to neat A-Zn during the 180 min, A/sCH-Ca film underwent more than 50% weight loss just after 60 min. This could be explained considering that the zinc ions, able to crosslink G as well as M and MG blocks, gave rise to a more complex network, in which the sCH chains were tightly entrapped; in addition, as previously mentioned (Pillay & Fassihi, 2005), the crosslinking with zinc, involving a greater number of ions, markedly delayed the sodium-zinc exchange rate. On the contrary, the high specificity of calcium towards G block implied a reduced number of ions and, as a consequence, a fast failing of the network was caused, with the hasty release of free chains. Nevertheless, at longer time A/sCH-Zn showed a drop in stability, resulting to be better indicated for short term dressings.

The addition of fibre (Fig. 2b) did not induce significant changes in A/F-Ca, A/F-Zn and A/sCH/F-Ca samples, while a slight improvement was found in the case of A/sCH/F-Zn blend. Furthermore, fibrous films showed a better physical stability at visual inspection.

3.3. Water vapour transmission rate (WVTR)

WVTR values of all samples are reported in Table 1. A film of plain sCH was also tested as a comparison. In agreement with Peppas (1987), the employment of hydrogels in wound dressing requires both the control of biological fluids loss from the wound site due to exudation and the maintenance of a moist environment over the wound bed, useful to enhance the regeneration of damaged epithelium. Bruin, Jonkman, Meijer, and Permings (1990) and El Salmawi

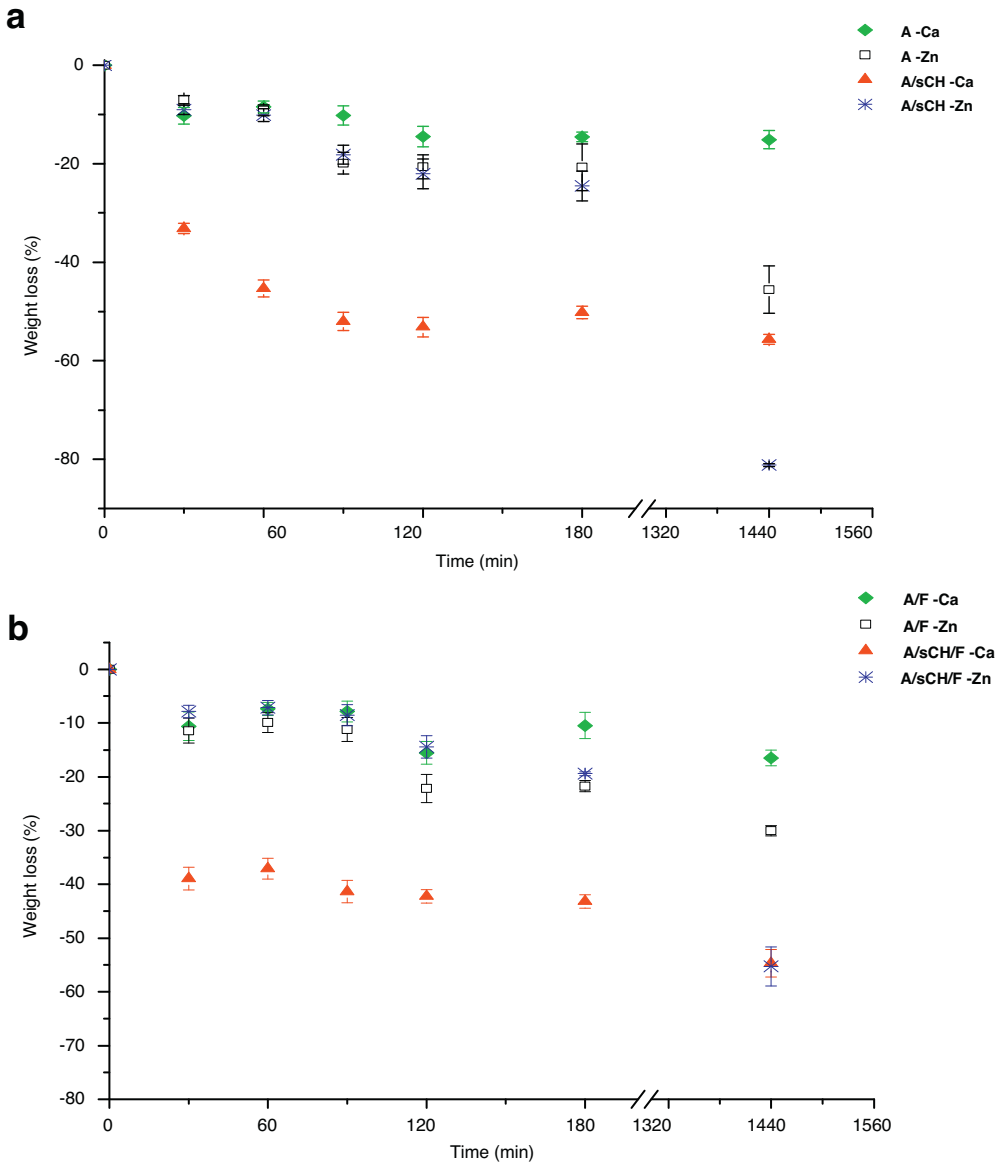

Fig. 2. Weight loss percentage ($\Delta W\,\%$) as a function of time (min) of films (a) and fibrous films (b) in saline solution.

Table 1
Water vapour transmission rate (WVTR), Young modulus (E), strain at break (σ), elongation at break (ε) of films and fibrous films.

Sample	WVTR [g (h m^2)$^{-1}$] ± 3%	Mechanical properties		
		E (MPa) ± 10%	σ (MPa) ± 10%	ε (%) ± 5%
A	42.65	3470	56.5	7.42
A/F	36.19	3628	58.9	2.95
sCH	45.01	1597	37.7	12.9
sCH/F	41.99	1678	43.5	12.2
A/sCH	43.93	2435	48.2	15.8
A/sCH/F	40.48	2514	47.7	14.4
A-Ca	39.70	3968	57.3	5.19
A/F-Ca	43.50	4123	60.2	4.58
A/sCH-Ca	37.30	2561	45.9	6.78
A/sCH/F Ca	35.20	2607	50.4	4.49
A-Zn	43.97	3526	48.1	7.23
A/F-Zn	42.13	3798	50.3	7.19
A/sCH-Zn	39.49	3014	53.1	8.32
A/sCH/F -Zn	35.67	3161	55.8	6.38

(2007) showed that, in order to avoid possible occlusive effects of wound coverings, WVTR must be higher than 33 [g(h m^2)$^{-1}$]; on the other hand, values over 53 [g(h m^2)$^{-1}$] supply a rapid exudation and evaporation of skin liquid, thus providing a detrimental drying effect of wound site. As a matter of fact, Table 1 shows that all samples ranged in a suitable interval of WVTR values, thus resulting potential candidates as wound dressing materials.

As concerning the un-crosslinked samples, it is meaningful to underline that sCH showed the higher WVTR, also when blended with sodium alginate (A/sCH). This outcome was probably due to the presence of bulky succinyl groups in sCH sample, able to decrease the macromolecular entanglements, favouring the water permeation throughout the films surface (Na, Wang, Wang, & Mao, 2013). Both plain A and blended films showed lowest WVTR values upon crosslinking. According to literature (Crank & Parker, 1968), this is a consequence of the formation of the junction zones, responsible of hindrance to water diffusion. It is worthwhile to underline that A-Zn sample evidenced higher WVTR values with respect to the other crosslinked samples. This outcome was attributed once again to the lack of selectivity of Zn^{2+} with respect to Ca^{2+}, that entailed less tight and stiff junction zones, resulting in a more flexible network. Fibrous films generally showed a reduction in WVTR, even if the values were still comprised in the optimal range. Cellulose microfibers strongly interact with A and sCH, probably providing a partial occlusive effect, not detrimental for the applicative purposes.

3.4. Mechanical properties

Mechanical properties of the films and fibrous films were summarized in Table 1. Young modulus (E) specifies the stiffness or rigidity of the film, strain at break (σ) indicates the tensile strength of the film to resist breaking and elongation at break (ε) describes the flexibility or extensibility of the films (Wu & McGinity, 2000). The analysis of the results indicated that, as expected, the addition of cellulose fibres induced a slight increase of Young modulus and stress at break values in all the tested samples, due to the formation of tightly hydrogen bonded networks between fibres and matrices, as previously underlined in the paper and confirmed also by Scanning Electron Microscopy analysis (see later). In addition, crosslinked films generally showed higher values of Young modulus if compared to the ones found in un-crosslinked samples, in this way resulting more rigid and less flexible (lower elongation at break percentage). Nevertheless, A/sCH based films showed an improved extensibility with respect to the plain polymers as evidenced by their higher percentage of elongation at break, even if crosslinked samples were considered. Moreover, the samples crosslinked with zinc ions are more flexible if compared to calcium crosslinked films, as evidenced by the higher strain at break values, confirming that overall networks junctions are less tight in the case of zinc.

3.5. Scanning electron microscopy (SEM)

SEM analysis was performed on the surfaces of fibrous films, to evidence dispersion and adhesion of fibres within polymeric matrices.

A picture of a cellulose microfiber (F) is reported in Fig. 3a. The fibre showed a smooth surface and homogeneous diameter size. The surface morphology of A/F, sCH/F, A/sCH/F samples was shown in Fig. 3b–e.

It is worthy to underline that the cellulose microfibers were well dispersed in both the polymeric matrices, providing the formation of a sort of fibrous texture. In particular, in A/F sample (Fig. 3b), the fibres were not perfectly covered by the polymer, while, in sCH/F sample (Fig. 3c), were homogeneously spread and well embedded into the sCH matrix, suggesting a stronger interaction.

Table 2
Effect of zinc on MSCs viability as a function of concentration.

Zn (μM)	RFU ± SD	Cell viability (%)
0	44 ± 1	100.0
12.5	43 ± 2	97.7
25.0	44 ± 1	100.0
50.0	43 ± 1	97.7
100	40 ± 2	90.9
200	30 ± 2	68.2
300	10 ± 1	22.7
400	4 ± 1	9.1

Upon crosslinking, a shrinkage of the surface was noticed, while no relevant differences were found between A/F-Ca and A/F-Zn films (micrographs not shown).

The adhesion of fibres to polymers worsened in A/sCH/F film with respect to the neat polymers (Fig. 3d and e), while upon crosslinking the fibres appeared well covered, and some differences arose between Ca and Zn crosslinked samples (Fig. 4a–d).

Microfibers were still clearly visible on the surface in A/sCH/F-Ca sample, while resulted highly incorporated within the polymeric network in A/sCH/F-Zn sample. This features is very appealing for clinical applications, as the fibres, being well covered by the hydrogels, should not neither stick to the wound bed or be absorbed by infected tissue, and thus should be easily removed by rinsing with physiological solution. As a result, the dressing change will be effortless, overcoming the drawbacks of common fibrous dressing.

3.6. Antibacterial activity

The antimicrobial effect against *E. coli* and *S. aureus* of the various zinc-crosslinked samples after 24 h contact time are reported in Fig. 5a and b, respectively. Calcium alginate hydrogel is reported as a control.

The reference concentration of bacteria is 5.5 and 6.0×10^6 CFU mL^{-1} for *E. coli* and *S. aureus*, respectively. The logarithmic reductions, after 24 h, are about of 2–3 orders of magnitude for *E. coli* and of about 2 orders for *S. aureus*, corresponding to a reduction upon to 99% CFU.

3.7. Atomic absorption spectrometry (AAS)

In Fig. 6 the kinetics release of zinc ions as a function of time is reported.

It is evident that all samples released more than 50% (w/v) of zinc within 20 min; moreover it must be emphasized that, after 60 min, fairly the totality of zinc content was found in solution, thus confirming that the ionic exchange was fast.

This outcome could play a key role in the formulation of antimicrobial wound dressing to be used on acute and chronic highly exuding wounds, where continuous wound cleansing treatments are requested in order both to inhibit the topical colonization of bacteria strains and to enhance the wound healing process (Flores& Kingsley, 2007; Kingsley, 2001). In these cases, a sustained and rapid release of zinc ions is desirable.

3.8. Cytotoxicity tests

In order to assess if the amount of zinc released from the hydrogels may cause toxic effects, toxicity of zinc at different concentrations was tested on MSC cells that are multipotent cells able to differentiate into a variety of phenotypes. After 24 h cell vitality was assessed by PrestoBlue test (Table 2).

From the obtained results it clearly appeared that up to 100 μM no cytotoxicity was evident, whereas cell viability was drastically

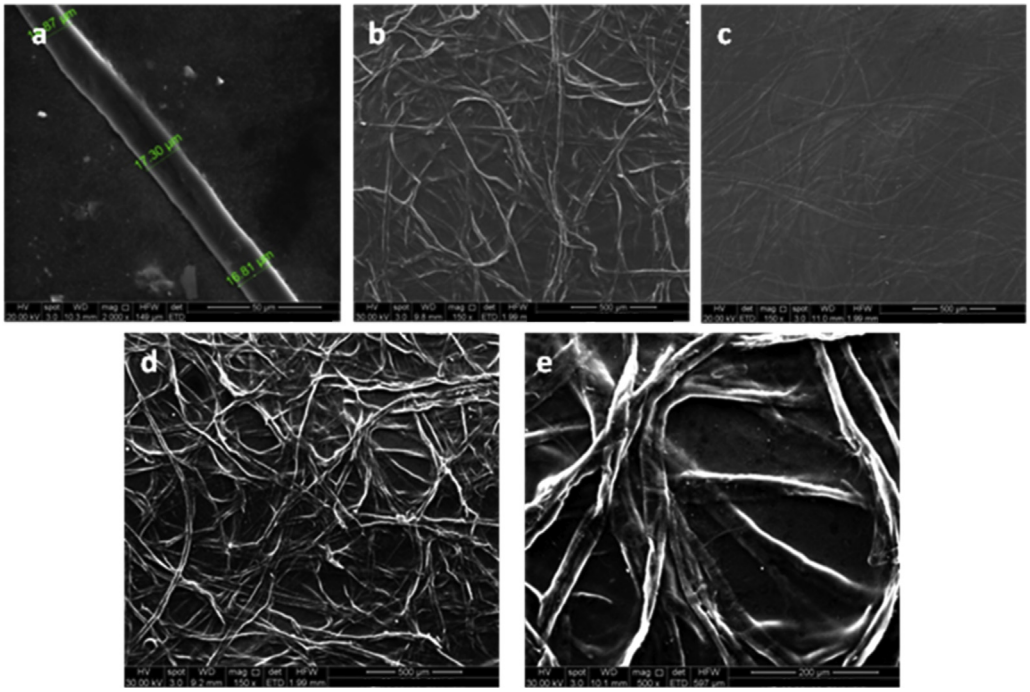

Fig. 3. SEM micrographs of cellulose microfiber F (a), A/F (b) and sCH/F (c) A/sCH/F un-crosslinked surface (d and e).

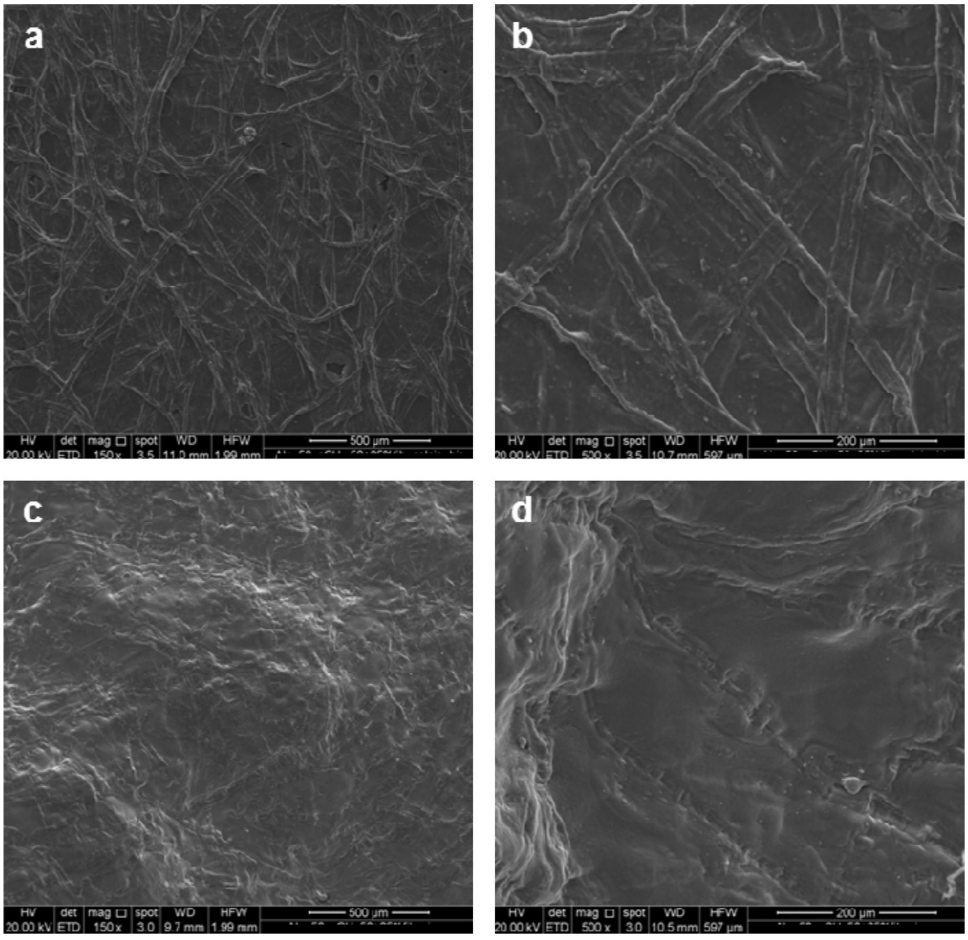

Fig. 4. SEM micrograph of A/sCH/F-Ca (a and b) and A/sCH/F-Zn (c and d) surfaces.

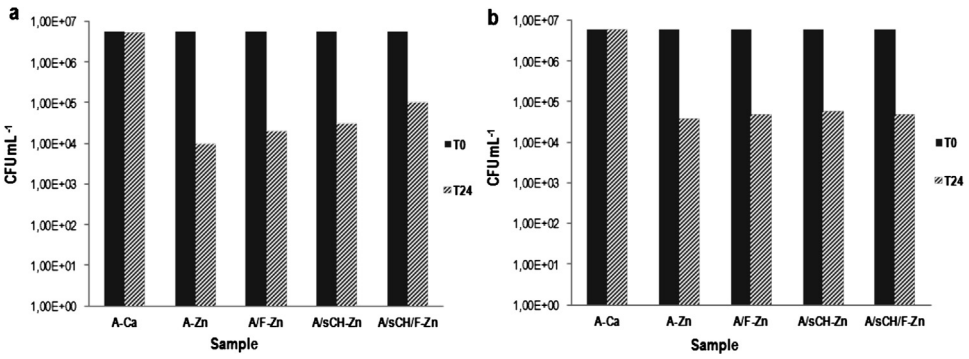

Fig. 5. CFU mL^{-1} reduction of *Escherichia coli* (a) and *Staphylococcus aureus* (b) in crosslinked samples as a function of contact time (*t*).

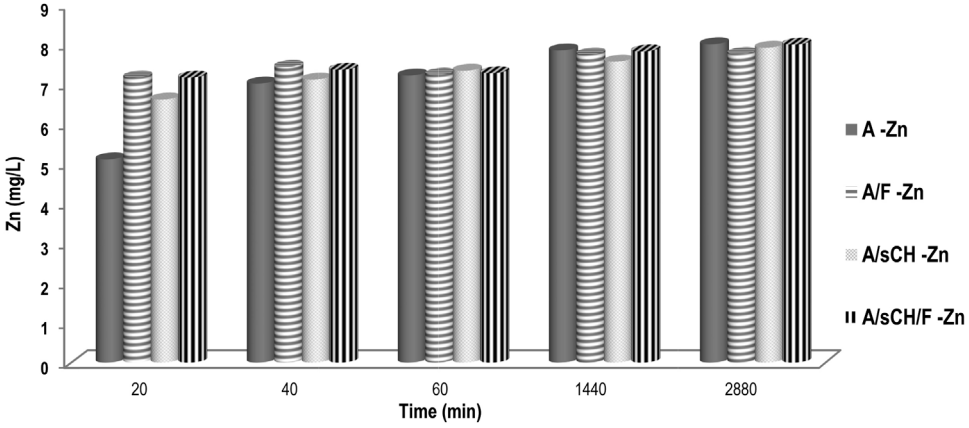

Fig. 6. Release kinetics of zinc ions in crosslinked samples.

reduced at 70%, 23% and 10% of the control at 200, 300 and 400 μM, respectively.

The concentration of zinc released from the hydrogels in RS solution, as measured by AAS (see previous paragraph), reached a maximum of 8 mg L^{-1}, which corresponds to 122 μM. At these concentrations a slight cytotoxic effect is elicited. Nevertheless, it is important to consider that the kinetics release of zinc depends on the surrounding medium, and that its local concentration could result to be lower in case of highly exuding lesions.

4. Conclusions

In this paper, hydrogels based on alginate and N-succinylchitosan blends, as such or containing microcellulose fibres, were prepared, crosslinked by either calcium or zinc ions and characterized, with the aim to explore on their potentiality in wound dressing. The presence of N-succinylchitosan considerably improved the properties of plain alginate hydrogels, by decreasing syneresis, enhancing swelling degree and improving water permeation, thus preserving a moist environment on the wound bed. Moreover, all these properties were enhanced when crosslinking was performed with zinc ions. The addition of cellulose microfibers provided only a slight decrease of swelling degree and WVTR values. SEM analysis showed a better embedding of fibres within the polymeric matrices in the case of hydrogels containing sCH, useful to prevent sticking of the fibres to wound bed and thus supporting the dressing change. Furthermore, the zinc-crosslinked hydrogels showed antibacterial activity against two common skin pathogens, *S. aureus* and *E. coli*, evidencing a reduction upon to 99% of bacteria colony-forming units after 24 hours of contact time. Cytotoxicity assays on MSCs cells allowed to establish that the amount of zinc released is slightly over the toxic level.

On the basis of experimental results, A/sCH/F-Zn resulted to be the formulation that better matched the various properties, as it showed high swelling associated to low shrinkage, good water vapour transmission rate, short-term stability in physiological medium, better flexibility, excellent fibres embedding, fast zinc release and sustained antibacterial activity. Nevertheless, to be proposed for wound dressing it is necessary to deeply investigate on the zinc release kinetics in the wound surrounding medium, and to establish if the concentration of zinc released could really cause a damage to the lesion.

Acknowledgements

The authors gratefully acknowledge the project DIATEME, in the frame of National Operative Program (PON 2007–2013), for the research financial support. They would like to thank Dr. Mario Malinconico for the valuable scientific advices, and the laboratory of electron microscopy “LaMEST” CNR, in the person of Maria Cristina Del Barone for the kind technical assistance in performing SEM analysis.

Appendix A. Supplementary data

Supplementary data associated with this article can be found, in the online version, at http://dx.doi.org/10.1016/j.carbpol.2014.02.054.

References

Abdelrahman, T., & Newton, H. (2011). Wound dressing: Principles and practice. *Wound Management*, *29*(10), 491–495.

Aslani, P., & Kennedy, R. A. (1996). Effect of gelation conditions and dissolution media on the release of paracetamol from alginate gel bead. *Journal of Microencapsulation*, *13*, 601–614.

ASTM E96. (1993). *Standard test methods for water vapour transmission of materials*. Philadelphia: American Society or Testing and Materials.

ASTM E 2149-01. (2001). *Standard test method for determining the antimicrobial activity of immobilized antimicrobial agents under dynamic contact conditions*. Philadelphia: American Society or Testing and Materials.

Boateng, J. S., Matthews, K. H., Stevens, H. N. E., & Eccleston, G. M. (2008). Wound healing dressings and drug delivery systems: A review. *Journal of Pharmaceutical Sciences*, *97*(8), 2892–2923.

Bruin, P., Jonkman, M. F., Meijer, H. J., & Permings, A. J. (1990). A new porous polyether urethane wound covering. *Journal of Biomedical Materials Research*, *24*, 217–226.

Chan, A. W., Whitney, R. A., & Neufeld, R. J. (2009). Semisynthesis of a controlled stimuli-responsive alginate hydrogel. *Biomacromolecules*, *10*, 609–616.

Chan, L. W., Jin, Y., & Heng, P. W. S. (2002). Crosslinking mechanisms of calcium and zinc in production of alginate microspheres. *International Journal of Pharmaceutics*, *242*, 255–258.

Crank, J., & Parker, G. S. (Eds.). (1968). *Diffusion in polymers*. New York: Academic Press.

Davidovich-Pinhas, M., & Bianco-Peled, H. (2010). A quantitative analysis of alginate swelling. *Carbohydrate Polymers*, *79*, 1020–1027.

Donaghue, V. M., Chrzan, J. S., Rosemblum, B. I., Giurini, J. M., Habershaw, G. M., & Veves, A. (1998). Evaluation of collagen-alginate wound dressing in the management of diabetic foot ulcers. *Advanced Wound Care*, *11*(3), 114–119.

Doyle, J. W., Roth, T. P., Smith, R. M., Li, Y. Q., & Dunn, R. M. (1996). Effects of calcium alginate on cellular wound healing processes modelled in vitro. *Journal of Biomedical Material Research*, *32*, 561–568.

Draget, K. I., Gaserod, O., Aune, I., Andersen, P. O., Storbakken, B., Stokke, B. T., et al. (2001). Effects of molecular weight and elastic segment flexibility on syneresis in Ca-alginate gels. *Food Hydrocolloids*, *15*(4–6), 485–490.

Draget, K. I., Oestgaard, K., & Smidsroed, O. (1990). Homogeneous alginate gels: A technical approach. *Carbohydrate Polymers*, *14*(2), 159–178.

El Salmawi, K. J. (2007). Gamma radiation-induced crosslinked PVA/chitosan blends for wound dressing. *Journal of Macromolecular Science, Part A: Pure and Applied Chemistry*, *44*(5), 541–545.

Flores, A., & Kingsley, A. (2007). Topical antimicrobial dressings: An overview. *Wound Essential.*, *2*, 182–185.

Goh, C. H., Heng, P. W. S., & Chan, L. W. (2012). Cross-linker and non-gelling Na^+ effects on multi-functional alginate dressings. *Carbohydrate Polymers*, *87*, 1796–1802.

Gomez d'Ayala, G., De Rosa, A., Laurienzo, P., & Malinconico, M. (2007). Development of a new calcium sulphate-based composite using alginate and chemically modified chitosan for bone regeneration. *Journal of Biomedical Materials Research Part A*, *81*(4), 811–820.

Grace, M., Chand, N., & Bajpai, S. K. (2009). Copper alginate-cotton cellulose (CACC) fibers with excellent antibacterial properties. *Journal of Engineered Fibers and Fabrics*, *4*, 24–35.

Grant, G. T., Morris, E. R., Rees, D. A., Smith, P. J. C., & Thom, D. (1973). Biological interactions between polysaccharides and divalent cations. Egg-box model. *FEBS Letters*, *32*(1), 195–198.

Hoffman, A. S. (2012). Hydrogels for biomedical applications. *Advanced Drug Delivery Reviews*, *64*, 18–23.

Hyun-Jung, C., Kyung-Soo, W., & Seung-Taik, L. (2004). Glass transition and enthalpy relaxation of cross-linked corn starches. *Carbohydrate Polymers*, *55*, 9–15.

Jay, S. M., & Saltzman, W. M. (2009). Controlled delivery of VEGF via modulation of alginate microparticle ionic crosslinking. *Journal of Controlled Release*, *134*(1), 26–34.

Karaaslan, M. A., Tshabalala, M. A., & Buschle-Diller, G. (2012). Semi-interpenetrating polymer network hydrogels based on aspen hemicellulose and chitosan: Effect of crosslinking sequence on hydrogel properties. *Journal of Applied Polymer Science*, *124*(2), 1168–1177.

Khan, A. T., Peh, K. K., & Ch'ng, A. S. (2000). Mechanical bioadhesive and biological evaluations of chitosan films for wound dressing. *Journal of Pharmaceutical Science*, *3*, 303–311.

Kingsley, A. (2001). A proactive approach to wound infection. *Nursing Standard*, *15*, 50–58.

Kong, H. J., Lee, K. Y., & Mooney, D. J. (2003). Non destructively probing the crosslinking density of polymeric hydrogels? *Macromolecules*, *36*(20), 7887–7890.

Kong, M., Chen, X. G., Xing, K., & Park, H. Y. (2010). Antimicrobial properties of chitosan and mode of action: A state of the art review. *International Journal of Food Microbiology*, *144*, 51–63.

Lansdown, A. B. (2002). Calcium: A potential central regulator in wound healing in the skin. *Wound Repair Regeneration*, *10*, 271–285.

Lay-Flurrie, K. (2004). The properties of hydrogel dressings and their impact on wound healing. *Professional Nurse*, *19*, 269–273.

Li, Ping., Dai, Ya-Ni., Zhang, Jun-Ping., Wang, Ai-Qin., & Wei, Qin. (2008). Chitosan-alginate nanoparticles as a novel drug delivery system for nifedipine. *Journal of Biomedical Science*, *4*(3), 221–228.

Muzzarelli, R. A. A. (2009). Chitins and chitosans for the repair of wounded skin, nerve cartilage and bone. *Carbohydrate Polymers*, *76*, 167–182.

Na, L., Wang, J., Wang, L., & Mao, S. (2013). A novel permeation enhancer: N-succinyl chitosan on the intranasal absorption of isosorbidedinitrate in rats. *European Journal of Pharmaceutical Sciences*, *48*(1-2), 301–306.

Na, S. Y., Oh, S. H., Song, K. S., & Lee, J. H. (2012). Hyaluronic acid/mildly crosslinked alginate hydrogel as an injectable tissue adhesion barrier. *Journal of Materials Science: Materials in Medicine*, *23*(9), 2303–2313.

Nobile, M. R., Pirozzi, V., Somma, E., Gomez d'Ayala, G., & Laurienzo, P. (2008). Development and rheological investigation of novel alginate/N-succinylchitosan hydrogels. *Journal of Polymeric Science. Part B, Polymer Physics*, *46*, 1167–1182.

Oliva, A., Passaro, I., Di Pasquale, R., Di Feo, A., Criscuolo, M., Zappia, V., et al. (2005). Ex vivo expansion of bone marrow stromal cells by platelet-rich plasma: A promising strategy in maxillo facial surgery. *International Journal of Immunopathology and Pharmacology*, *18*, 47–53.

Omidian, H., Rocca, J. G., & Park, K. (2006). Elastic, superporous hydrogel hybrids of polyacrylamide and sodium alginate. *Macromolecular Bioscience*, *6*(9), 703–710.

Ovington, L. G. (2007). Advances in wound healing. *Clinical Dermatology*, 25–33.

Pandima Devi, M., Sekar, M., Chamundeswari, M., Moorthy, A., Krithiga, G., Selva Murugan, N., et al. (2012). A novel wound dressing material fibrin chitosan sodium alginate composite sheet. *Bulletin of Material Science*, *35*(7), 1157–1163.

Peng, C. W., Lin, H. Y., Wang, H. W., & Wu, W. W. (2012). The influence of operating parameters on the drug release and anti-bacterial performances of alginate wound dressings prepared by three-dimensional plotting. *Materials Science and Engineering C*, *32*(8), 2491–2500.

Peppas, N. A. (1987). . N. A. Peppas (Ed.), *Hydrogels in medicine and pharmacy* Boca Raton, FL: CRC Press Inc.

Pillay, V., & Fassihi, R. (2005). Novel modulation of drug delivery using binary zinc-alginate-pectinate polyspheres for zero-order kinetics over several days: Experimental design strategy to elucidate the crosslinking mechanism. *Drug Development and Industrial Pharmacy*, *31*, 191–207.

Pudner, R. (2001). Amorphous hydrogel dressings in wound management. *Journal of Community Nursery*, *15*(6), 43–46.

Raghavendr, G. M., Jayaramudu, T., Varaprasad, K., Sadiku, R., Ray, S. S., & Raju, K. M. (2013). Cellulose–polymer–Ag nanocomposite fibers for antibacterial fabrics/skin scaffolds. *Carbohydrate Polymers*, *93*(2), 553–560.

Russo, R., Malinconico, M., & Santagata, G. (2007). Effect of cross-linking with calcium ions on the physical properties of alginate films. *Biomacromolecules*, *8*, 3193–3197.

Sakchai, W., Churrerat, P., & Srisagul, S. (2006). Development and in vitro evaluation of chitosan-eudragit RS 30D composite wound dressings. *AAPS PharmSciTech*, *7*, E1–E6.

Stokke, B. T., Draget, K. I., Smidsrod, O., Yuguchi, Y., Urakawa, H., & Kajiwara, K. (2000). Small-angle X-ray scattering and rheological characterization of alginate gels. 1. Calcium alginate gels. *Macromolecules*, *33*(5), 1853–1863.

Thomas, A., Harding, K. G., & Moore, K. (2000). Alginates from wound dressings activate human macrophages to secrete tumour necrosis factor-a. *Biomaterials*, *2*, 1797–1802.

Van Vlierberghe, S., Dubruel, P., & Schacht, E. (2011). Biopolymer-based hydrogels as scaffolds for tissue engineering applications: A review. *Biomacromolecules*, *12*, 1387–1408.

Werner, S., & Grose, R. (2003). Regulation of wound healing by growth factors and cytokines. *Physiological Reviews*, *83*, 835–870.

Wu, C., & McGinity, J. W. (2000). Influence of relative humidity on the mechanical and drug release properties of theophylline pellets coated with an acrylic polymer containing methylparaben as a non-traditional plasticizer. *European Journal of Pharmaceutics and Biopharmaceutics*, *50*(2), 277–284.

Yamaguchi, R., Arai, Y., Itoh, T., & Hirano, S. (1981). Preparation of partially N-succinylated chitosans and their cross-linked gels. *Carbohydrate Research*, *88*, 172–175.